INTERNATIONAL JOURNAL OF ADVANCED ENGINEERING AND BUSINESS SCIENCES (IJAEBS)

Journal homepage: https://ijaebs.journals.ekb.eg

Finite Element Modeling of RC Beams Repaired and Strengthened Using Jackets of Cementitious Materials and Subjected to Elevated Temperatures

Yasmin Hefni Abd El Aziz[1] and Mona Mostafa Abdel Wahab[2]

[1] *Civil Engineering Department - Faculty of Engineering-Modern University for Technology & Information, Cairo*

2 Department of Structural Engineering, Faculty of Engineering, Ain Shams University El Sarayat Street, Abbasia, Cairo

**Corresponding author:* yassmin.hefny@eng.mti.edu.eg

Received: 22-11-2022 **Accepted:** 06-05-2023 **Published**: 05-06-2023

ABSTRACT

This research aims towards presenting an appropriate model for analyzing reinforced concrete (RC) beams repaired and strengthened using jackets of cementitious materials.

The jackets incorporated chemically activated fly ash with glass fiber to enhance the load carrying capacity, cracking load and ductility at normal temperature and after exposed to elevated temperature. Three-dimensional nonlinear finite element (FE) model has been developed using finite element package, ANSYS 14.0. Eleven RC beams strengthened using plain or RC jackets containing activated fly ash and glass fibers and loaded with four-point loading arrangement were analyzed. The parameters of the study comprised damage level induced before jacketing, effect of exposure to elevated temperature and effect of jacket reinforcement. The finite element results obtained in this investigation; ultimate flexural capacity, mid-span deflection, crack progression, failure mode and stresses in concrete, showed good agreement when compared with the available experimental data results. The presented FE models showed the potential of performing numerical simulation instead of experimental tests to save time and costs.

Key words: Finite element model, RC Beams, Jackets, ANSYS 14.0.

1 INTRODUCTION

Jacketing of structural elements is a favorite solution to strengthening problems of old RC structures. Jackets have been created using traditional or precast concrete, steel and FRP wrapping [1,2,3, 16]. In spite of jacketing increases the member size significantly, it increases the stiffness, improves the load carrying capacity [3] and improves the fire resistance.

FE nonlinear analysis modeling is one of the widely applied methods to the concrete structures in predicting and understanding the response of these structures to various loadings. There are many methods for modeling RC structures using both analytical and numerical methodologies. FE nonlinear analysis modeling can simulate and forecast the strains and stresses of RC sections and reinforcement. Several FE commercial analysis codes exist along with the advanced modules for difficult analyses. Progressing knowledge and ability of computer package and hardware enlarged using FE.

ANSYS program is a good tool to predict the temperature distribution and thermal stresses through RC concrete sections [4,5,6,7,8, 17, 18]. Hsu and Lin [4] performed thermal and structural analyses to assess the residual bearing capabilities and flexural capacities of RC beams after fire by using ANSYS. Moetaz et al. [5] used ANSYS to confirm the numerical model by their experimental study of RC beams exposed to a controlled fire at 650° C. The beams were tested to failure after cooling to room temperature and the experimental results showed good agreement with the numerical modeling.

Jacob et al. [6] compared between fire resistance ratings predicted from IS 456: 2000 [9] and ANSYS thermal analysis, for beams with cross section 20 cm x 40 cm exposed to ISO 834 standard fire from two lateral sides and bottom sides. Heat was transferred from fire to element by convection on line with a convection film coefficient of 25W/m^{2}K. FE plane 55 was used for modeling concrete; it has a single degree of freedom with four nodes; temperature at each node. It was concluded that the used element is applicable for a two dimensional, steady-state or transient thermal analysis where good agreement was obtained between IS 456: 2000 [9] data and ANSYS thermal analysis.

2 Research significance

This study aims to present a FE model by using ANSYS program suitable for analyzing RC beams repaired and strengthened using jackets of activated fly ash (FA) and glass fibers (GF) and exposed to elevated temperature according to ASTM E119 fire rating curve. The incorporating ratio of activated fly ash was 40% and glass fiber was 0.7 % by weight of cement to enhance the load carrying capacity, cracking load and ductility at normal temperature and after exposed to elevated temperature. The parameters for the numerical analysis include beam dimensions, reinforcement,

materials properties, loading scheme, ultimate flexural capacity. The data obtained from the experimental investigation previously performed [10] was used to verify the accuracy of the presented finite element model.

3 Finite Elements Modeling

3.1 Finite element types

In this study, ANSYS FE type SOLID 65 represented concrete elements in beams and jackets. This element type has eight nodes and three degrees of freedom at each node (translations u, v, and w in the nodal x, y and z directions respectively) [11, 12]. This element is able to treat with nonlinear material properties and predicts the failure of the concrete material. In addition, it accounts for both cracking and crushing modes and also indicates plastic deformation and creep of concrete. Geometry, node locations, and the coordinate system for the element are shown in Figure 1 [11].

Reinforcement of beams and jackets are represented by ANSYS FE type LINK180. This element has the ability to pattern the behavior of stirrups in resisting the vertical shear and main steel reinforcement in resisting the flexural stresses. This element is a uniaxial tension-compression element with three degrees of freedom at each node (translation in the nodal x, y, and z directions). As in a pin-jointed structure, no bending of the element is considered. The geometry, node locations, and the coordinate system for the element are shown in Figure 2 [11].

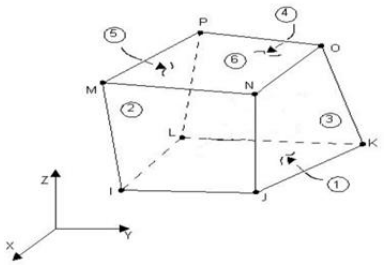

Figure 1: ANSYS finite element type Solid 65 (Concrete element) [11]

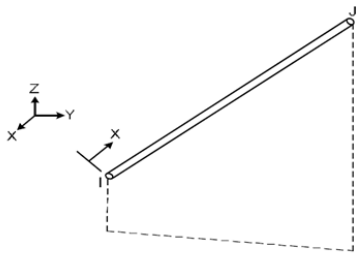

Figure 2: ANSYS finite element type Link 180 (reinforcement element) [11]

No contact elements were used to simulate the contact between the original beam and jacket; a full bond is assumed between the original beam and jacket since the surface of the original beams was chipped, roughened, and cleaned before casting the concrete jacket; also, adhesions and shear dowels were used to contact the jacket and original beam. Additionally, it was assumed that the new stirrups and dowels would be fully bonded to the original beam.

Manual direct generation technique was used in building 3D beam models. These 3D models were generated by defining all nodes which simulate the global building structure in the three spatial co-ordinate directions. Different element types of the structural members were generated using the

nodes defined previously. The model meshing was carried out using the free mesh technique (an ANSYS mesh technique) which allows the modeler to choose the appropriate finite element size.

The stress-strain curves for concrete and reinforcement are illustrated in Figures 3, 4. To define concrete and reinforcement elements for beams and jackets material properties such as Young's modulus, Poisson's ratio, density, strength are required. Depending on the desired type of structural analysis, the material properties can be linear or nonlinear. Regarding the nonlinear analysis, material properties can be orthotropic or anisotropic.

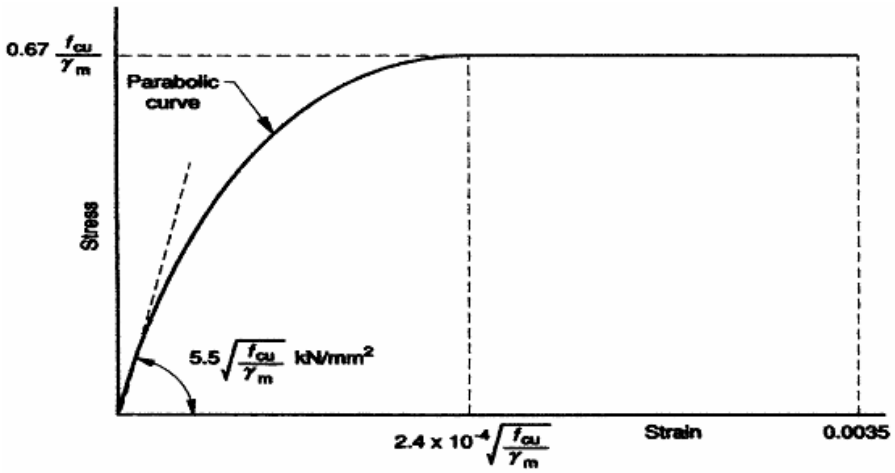

Figure 3: Short-term design stresses - strain curve represented normal-weight concrete (f_{cu} in N/mm^2) [11]

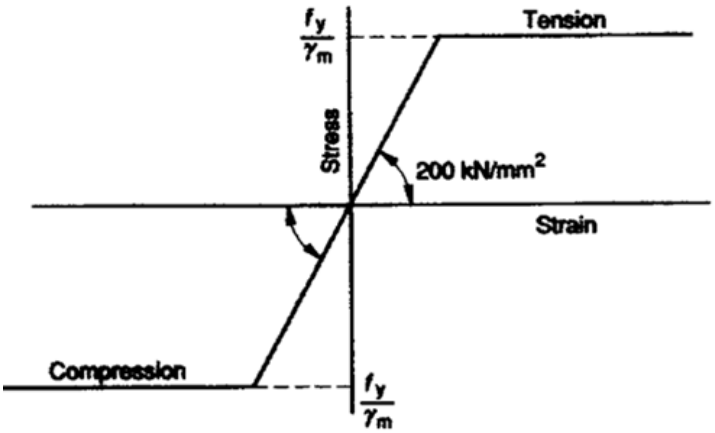

Figure 4: Short-term design stresses - strain curve represented steel reinforcement (f_y in N/mm^2) [11]

3.2 Concrete Failure Principles

Ultimate uniaxial compressive and tensile strengths are essential to explain the failure surface for concrete. Therefore, a principle for failure of concrete due to a multi-axial stress state is defined. Failure principles for multi-axial and biaxial states of stresses are illustrated in Figure 5 and 6, respectively [12,13,14].

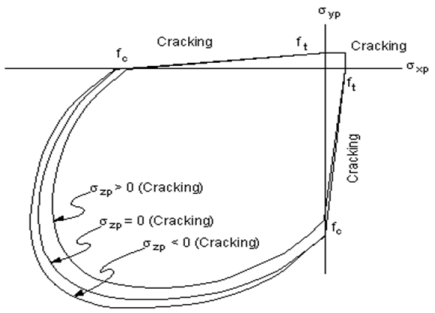

Figure 5: Failure surface in principal stress space in biaxial state of stresses

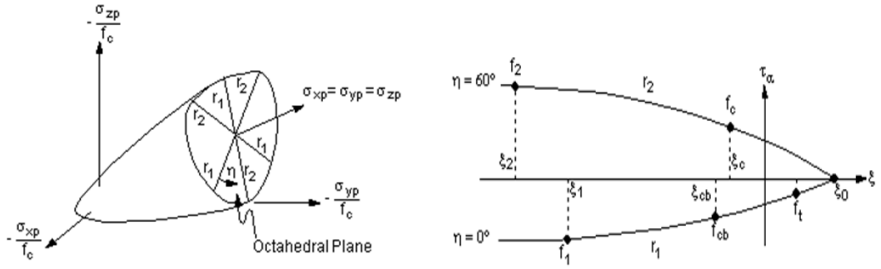

Figure 6: Three-dimensional failure surface and profile

3.3 Description of numerical models

Eleven three-dimensional FE models were performed. One of them represented a control beam. The beam was loaded to failure to find out the load carrying capacity and the corresponding deflection. The remaining 10 models represented strengthened beams using reinforced or plain concrete jackets. Some beams were preloaded to 65% of the ultimate load of control beam before jacketing. The material used for the jackets was either traditional concrete (Control mix) or concrete containing activated fly ash and glass fibers (GAF mix). Beams and jackets geometry, material properties and loading scheme of the constructed models are assumed similar to those of the experimental study previously presented by the author [10]. Table 1 illustrates the description of numerical models.

Table 1: Description of the numerical models

Beam No.[10]	Preloading	Elevated Temperature.	Jacket Type		Jacket Material	
			Reinforced.	Un Reinforced	Control	GAF
B1	-	-	-	-	-	-
B2	-	-	√	-	√	-
B3	-	-	√	-	-	√
B4	-	√	√	-	√	-
B5	-	√	√	-	-	√
B6	√	-	√	-	√	-
B7	√	-	√	-	-	√
B8	√	√	√	-	√	-
B9	√	√	√	-	-	√
B10	-	-	-	√	√	-
B11	-	-	-	√	-	√

3.3.1 Beams and jackets models geometry

The original beams were of span 225 cm and cross-section of 10 cm x 20 cm. The beams were reinforced with 2 T12 mm with grade 400 in tension and 2 T10 mm in compression and tided with stirrups R8@200 mm at the middle third and R8 @ 100 mm near supports. The RC jackets were three sides with 50 mm thickness for each side. The final dimensions of the jacketed beams were 20 cm x 25 cm x 225 cm. Reinforced jackets had 2 T10 mm and 2 T12 mm top and bottom reinforcement with grade 360, respectively, and tided with planted stirrups R8@20 cm at the middle third and R8@10 cm near the supports. Figure 7 shows the details of the modeled beams.

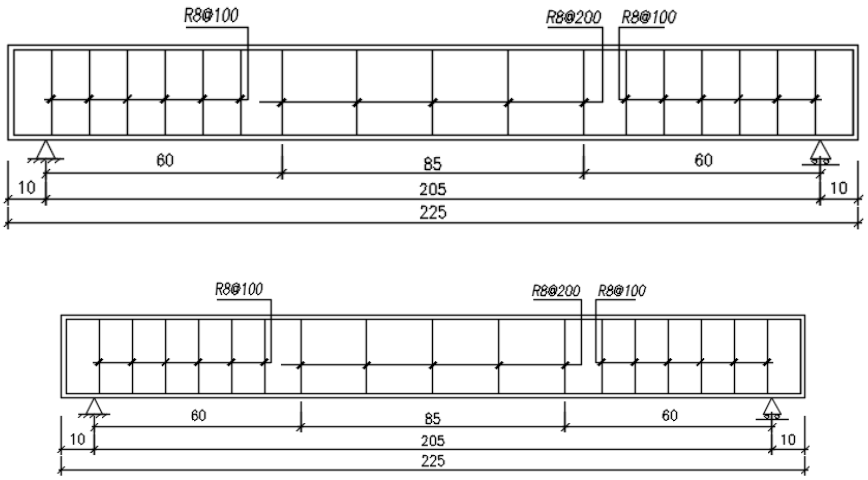

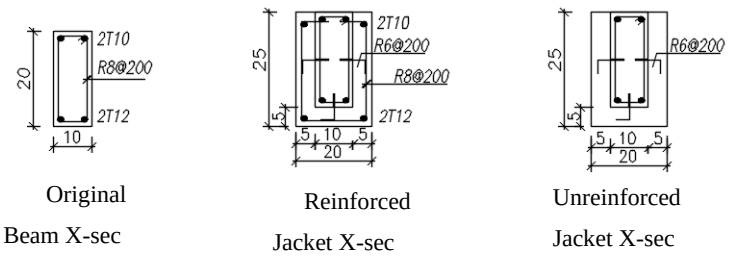

Figure 7: Dimensions (cm) and details of reinforcement for the molded

3.3.2 Three-dimensional FE models for beams and jackets

Figures 8 and 9 show FE model of the original beam generated using ANSYS program, whereas Figures from 10 to 13 show FE model of the strengthened beams.

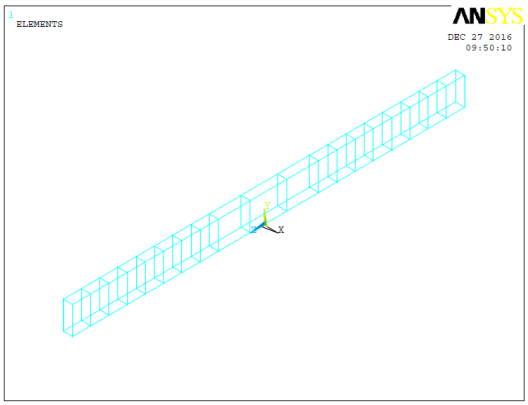

Figure 8: FE model for the original beam reinforcement

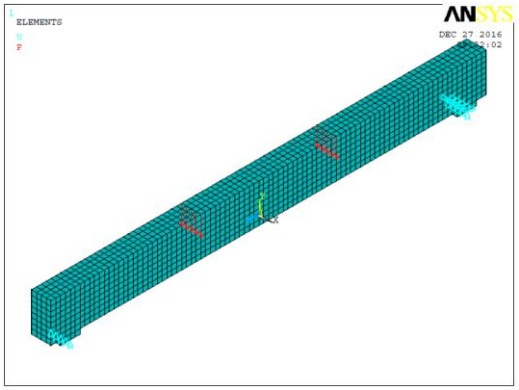

Figure 9: FE model for the original beam

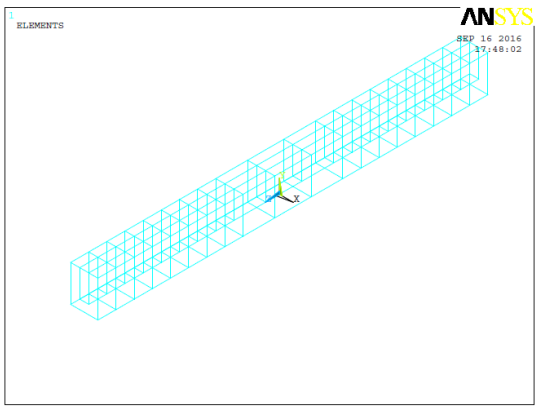

Figure 10: FE model for reinforcement of strengthened beam by using reinforced jackets

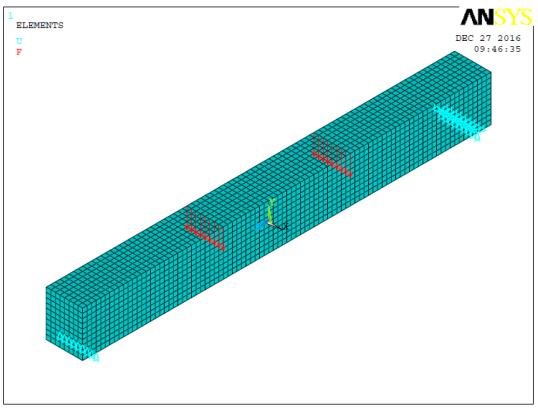

Figure 11: FE model for strengthened beam by using reinforced jackets

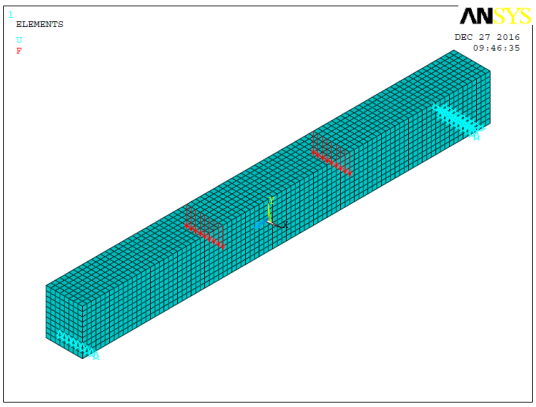

Figure 12: FE model for strengthened beam by using unreinforced jackets

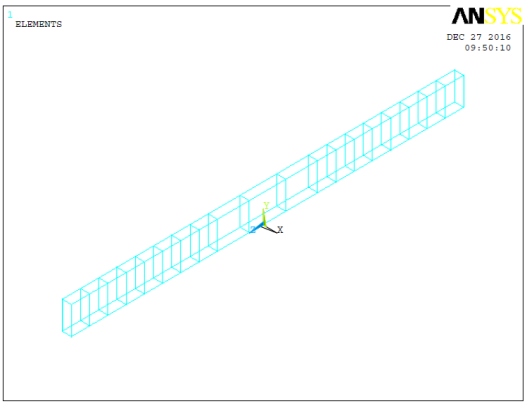

Figure 13: FE model for reinforcement of strengthened beam by using unreinforced jackets

3.3.3 Materials properties

All properties for concrete and reinforcement for modeled beams and jackets are taken based on the experimental study performed by the author [10].

3.3.3.1 Properties of concrete and reinforcement at normal temperature

Table 2 shows properties of concrete and reinforcement for control and strengthened beams at normal temperature.

Table 2 Properties of concrete and reinforcement at normal temperature [10]

Material type	Property	Original beam	Jackets of control mix	Jackets of GAF mix
Concrete	Compressive strength (N/mm^2)	30	25	35
	Tensile strength (N/mm^2)	3.3	2.6	3.3
	Young's modulus (E_c) (N/mm^2)	2.4e5	2.3e5	2.3e5
	Poisson's ratio (ν_c)	0.2	0.2	0.2
	Density (ρ_c) (kg/m^3)	2350	2350	2100
Steel Reinforcement	Yield strength (fy) (N/mm^2)	420	370	370
	Young's modulus (E_s) (N/mm^2)	2e6	2e6	2e6
	Poisson's ratio (ν_s)	0.3	0.3	0.3
	Poisson's ratio (ν_{frp})	0.27	0.27	0.27
	Density (ρ_s) (kg/m^3)	7850	7850	7850

3.3.3.2 Material properties for concrete and reinforcement after exposure to elevated temperature

- **Concrete**

Concrete strength for strengthened beams that were exposed to elevated temperature was estimated based on the measured temperature distribution through the beam cross section[10]. Beams and jackets cross section was divided into layers, the concrete strength based on the temperature rise at each layer location was determined as given in Table 3.

Table 3 Concrete strength for beams and jackets at different temperatures [10]

Concrete type	Original beams (180 days)				Jackets of control mix (56 days)				Jackets of GAF mix (56 days)			
Temp^{o} C	20 ^{o}	400 ^{o}	600 ^{o}	800 ^{o}	20 ^{o}	400 ^{o}	600 ^{o}	800 ^{o}	20 ^{o}	400 ^{o}	600 ^{o}	800 ^{o}
Compressive strength (N/mm^2)	30	21.5	18.5	7.0	25	21.0	15.68	5.0	35	29.75	25.6	12.0
Tensile strength (N/mm^2)	3.3	2.4	1.75	0.70	2.6	2.1	1.35	0.65	3.3	2.8	2.66	0.90
Young's Modulus (N/mm^2)x 10^3	24.00	12.10	6.20	2.20	23.00	11.24	6.15	2.20	23.00	10.80	5.00	2.19

- **Reinforcement**

Yield and tensile strengths for steel reinforcement of beams and jackets that were exposed to elevated temperature were applied at the numerical models based on Topcu and Karakurt study [10]. They concluded that lower yield and tensile strengths for steel reinforcement will attain better behavior of structure elements when exposed to elevated temperatures. Reinforcement lost almost its strength when the temperature at the reinforcement location exceeds 500 ^{o}C. Tensile and Yield strengths of reinforcement against temperature are illustrated in Figures 15 and 16 [15].

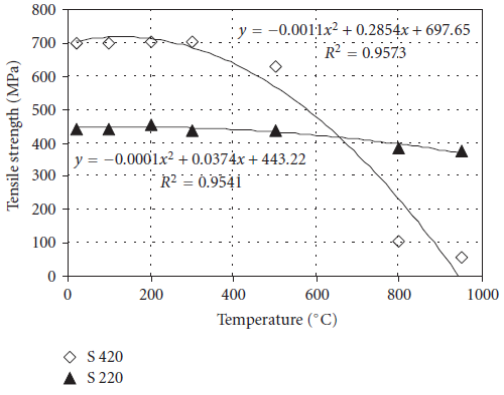

Figure 15: Tensile strength of reinforcement and temperature for steel grades S420 and S220 [15]

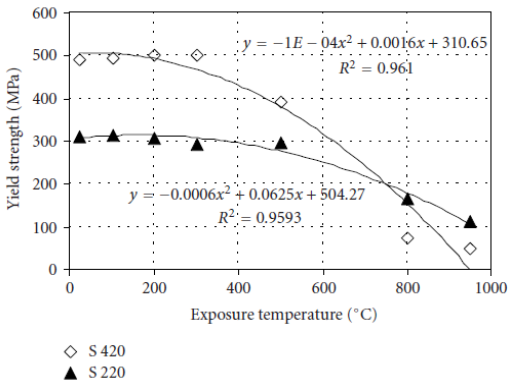

Figure 16: Yield strength of reinforcement and temperature for steel grades S420 and S220 [15]

3.3.4 Loading Scheme

The loading scheme of the beam models was typically similar to that of the experimental loading scheme [10]. The beam models were loaded in four points loading over a simply supported span with length of 205 cm as shown in Figure 17.

Control and strengthened beam models were loaded at one step till failure. Kill and birth options [7] were used to simulate the behavior of preloaded beams, in this option, the beams were loaded at the first step to 2/3 the ultimate load, and then concrete jacket and reinforcement were deactivated by killed option. The program gives stiffness multiplied factors to the killed elements near zero, after the first step. The killed elements will be activated by using birth option and the total load was applied on the preloaded beam.

After loading the beam models, the results of the numerical analysis are presented. These results include crack pattern, mid-span deflection and the failure modes.

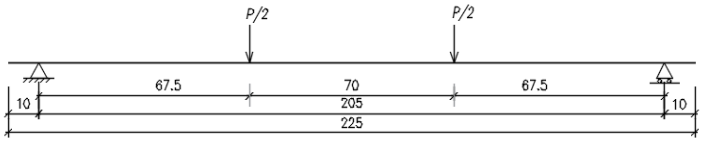

Figure 17: Loading scheme (dimensions in cm) [10]

3.3.5 Nonlinear Solution

In nonlinear analysis, a load increment defined as load steps is used to divide the total load in a FE model. At the end of incremental solution steps, the stiffness matrix of the model is used to mirror nonlinear changes in beam stiffness before proceeding to the next load steps. Newton–Raphson equilibrium iterations [3, 10] for updating the model stiffness were used in ANSYS program. In this study, for RC solid elements, convergence criteria were founded on displacement and force, and the convergence tolerance limits were primarily selected by the ANSYS program. It was found that convergence of solutions for the models was difficult to achieve due to the nonlinear behavior of RC. Therefore, the convergence tolerance limits were increased to a max of 5 times the default tolerance limits (0.5% for force checking and 5% for displacement checking) in order to obtain convergence of the solutions.

4 Results and Discussions

The results of the numerical analysis and verifications with the experimental test results [10] are presented and discussed in this section to show the advantage of performing numerical simulation instead of experimental tests in saving time and costs. The verifications include ultimate loads (P_{ult}), mid-span deflection (Δ_{ult}), load deflection curves and crack patterns. Table 4 illustrates ultimate loads (P_{ult}) and mid beam deflection (Δ_{ult}) for both numerical and experimental studies. Load deflection curves for beams are shown in Figures 18 to 24. Failure modes and crack patterns are shown in Figures 25 and 35.

Table 4: Summery of numerical and experimental study [10]

Beam No.	P_{ult} (KN)			Δ_{ult} (mm)		
	Experimental	Numerical	Difference %	Experimental	Numerical	Difference %
B1	71.0	65.8	-7.3	35.0	33.1	-5.43
B2	142.0	144.8	2.0	34.0	35.7	5.00
B3	165.0	166.7	1.0	50.0	48.2	-3.60
B4	77.0	77.8	1.0	40.0	43.3	8.25
B5	95.0	97.5	2.6	46.0	52.7	**14.57**
B6	134.0	152.2	13.6	31.0	42.7	37.74
B7	155.0	158.4	2.2	36.0	50.5	40.28
B8	75.0	77.8	3.7	38.0	40.1	5.53
B9	88.0	93.0	5.7	42.0	45.1	7.38
B10	79.0	84.7	7.2	35.0	44.6	27.43
B11	83.0	89.0	7.2	37.0	45.0	21.62

4.1 Load carrying capacity

As illustrated in Table 4, use of GFA mix in jackets shows superior performance compared to control mix at normal temperature and after exposure to elevated temperatures. As indicated in the numerical study, using reinforced Jackets with un-cracked beams increased the load carrying capacity at normal temperature compared with the control beam model by 153.0% and 120.0 % for GFA mix and control mix, respectively. These ratios were considerably affected when using unreinforced jackets to 35.3% and 28.7 %, respectively. These values showed good agreement when compared with the results of the experimental study.

Preloading of beams to 65% of the ultimate load of control beam model before strengthening with reinforced jackets had a limited effect on the behavior of repaired beams. This may be due to the fact that the stiffness of the jacket, regardless of the type of mix used, makes it the major part in

carrying the load compared with the original beam. This result was also clear in the experimental study.

As illustrated in Table 4, the ultimate load of control beam B1 obtained from the numerical study was less than that of the experimental study by 7.3% Whereas; the value for other beams of the numerical study exceeds by range from 1.0 to 13.6%.

Good agreement for the mid-span deflection between numerical and experimental study for beams (B1 to B3); a notable difference occurs for (B6 & B7); the first illustrates larger increment values were 37.27% and 40.28% for control mix and GFA mix, respectively. This difference may be due to the neglected preloaded deflection in the experimental study and also the full assumed contact between the original beam and the jacket.

The effect of elevated temperature was remarkable on the modeled beams. Ultimate loads in the numerical investigation For beams strengthened by reinforced jackets made of control mixes and GFA (B4, B5) were reduced by 46.0% and 41.5%, respectively compared to with beams (B2,B3). These values were limited for preloaded beams to 41.2% and 48.8%, respectively.

Comparing the deflection of the numerical study and the experimental study after exposed to elevated temperature, the first increased by ratio ranged from 5.5 to 14.6%. The contact surface also affected this ratio; the new concrete was partially damaged in GFA jacket but totally damaged in control jacket so the difference was small in control jackets compared with GFA.

4.2 Load deflection curves

Figures 18, 19, 20, 21 show load deflection curves for control and strengthened un-cracked beams. The curves were bilinear for all beams. Using reinforced jackets improved the rigidity and load carrying capacity. The rigidity of beams with reinforced jackets (B2 and B3) was comparable to a load value of 130 KN (first phase of the behavior), after which the repaired beams suffered from

excess cracking. The stiffness was higher for FA mix compared with control one due to the impact of GF and FA. The load deflection curves for the numerical finite element models are nearly identical with the experimental results which reflect good agreement with the experimental study.

Similar curves were obtained for preloaded strengthened beams as shown in Figure 20. Preloading showed a significant effect in decreasing the stiffness when using control mix jackets. The numerical and the experimental results were different. This may be due to the partial removal of cracks in the experimental study which did not attain in the numerical analysis. Also, the contact surface between the preloaded beams and jackets was assumed to be fully contacted at the numerical models. This results in lateral movement of the contact joints suddenly after birth option before reloading. Figure 21 indicates good agreement between the numerical and the experimental results.

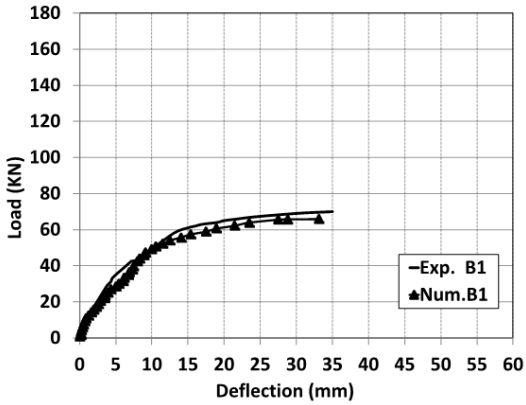

Figure 18: Load deflection curve for Control Beam

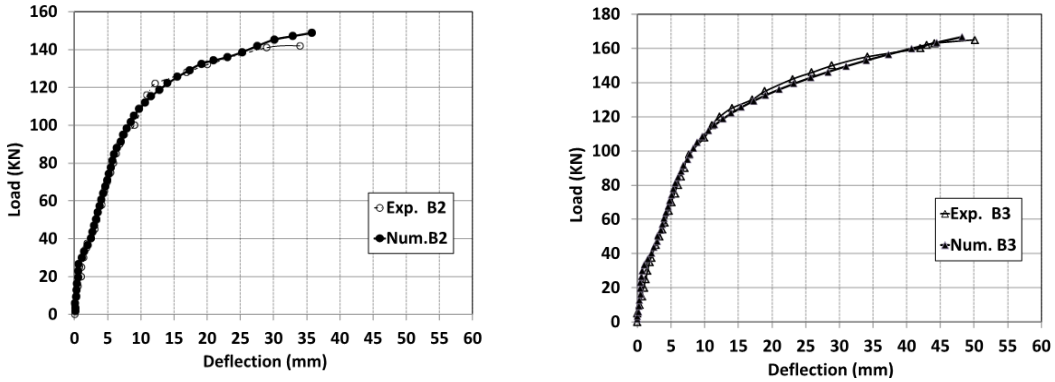

Figure 19: Load deflection curve for strengthened beams

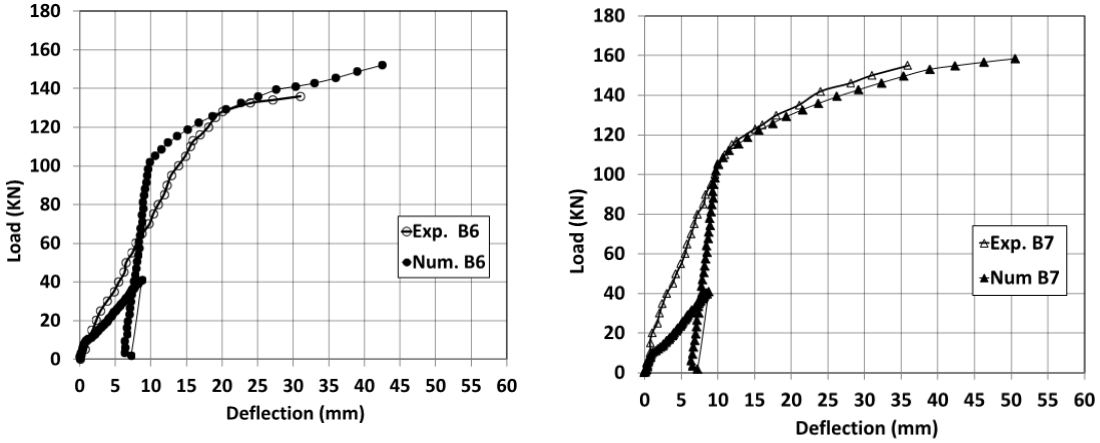

Figure 20: Load deflection curve for preloaded strengthened beams

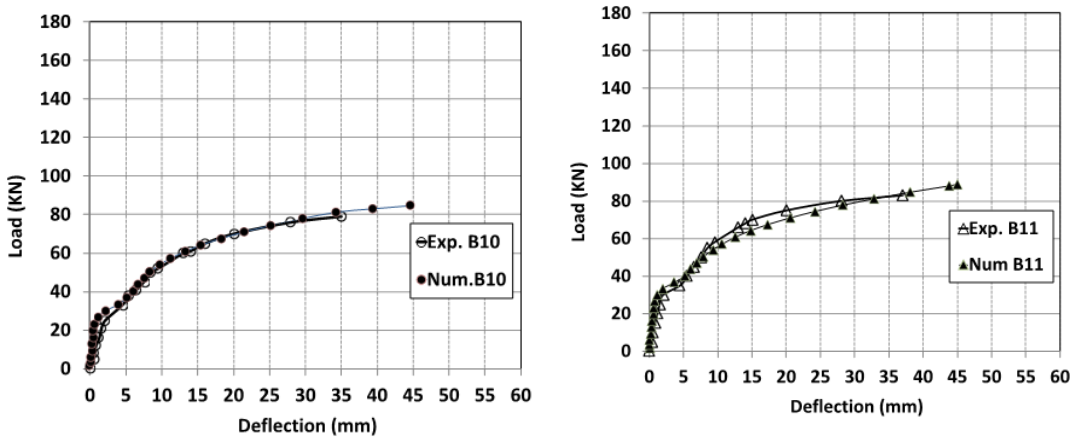

Figure 21: Load deflection curve for unreinforced strengthened beams

Figures 22 displays load deflection curves for strengthened un-cracked beams after exposure to elevated temperature, whereas Figures 23 displays those for preloaded beams. The significant distortion due to exposure to elevated temperature reduced the difference in the load carrying capacity between reinforced and unreinforced jackets. However, it was amazing for preloaded beams that use of unreinforced jacket made of FA mix showed identical behavior to reinforced jacket made of control mix. The credit is due to GF and FA effect in enhancing both stiffness and ultimate capacity. Figure 23 clarifies that the influence of the contact surface disappeared; this may be due to the weakness of the jacketed concrete and reinforcement which did not add a new valuable stiffness to the beam element.

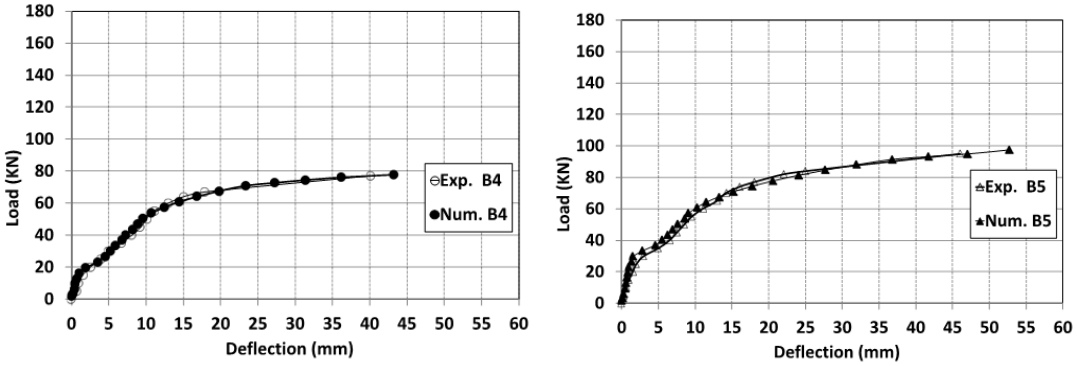

Figure 22: Load deflection curve for strengthened beams after exposure to elevated temperature

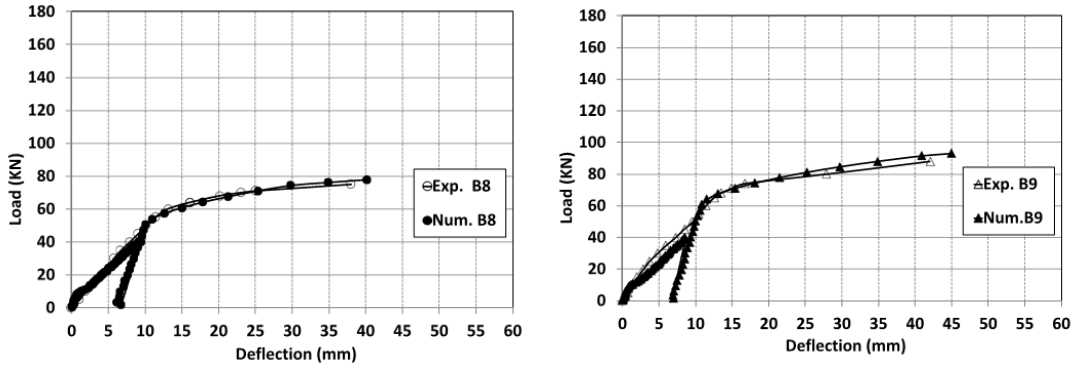

Figure 23: Load deflection curve for preloaded strengthened beams after exposure to elevated temperature

4.3 Crack progression

The cracking patterns in the beam can be obtained using the Crack/Crushing plot option in ANSYS. Vector Mode plots must be turned on to view the cracking in the model. Figures 24 to 34 show the progression of cracks and crushing in the FE models of control beam, strengthened and preloaded beams at different stages of loading (0.25, 0.5, 0.75 and 1.0) of P_{ult}. In order to better display the progression of cracking and crushing in (ANSYS). A circle outline in the plane of the crack represents cracking while an octahedron outline represents crushing. If a crack has opened and then closed, the circle outline will have an X through it. Each integration point can crack in up to three different planes. The first, second, and third crack at an integration point is shown with a red, green, and blue circle outline, respectively. It should be noted that even micro cracks and crushing are displayed and that it is not necessarily a progression of flexural or shear cracks. Crack progression

For experimentally loaded beams, Cracks may be either macro cracks, detectable by visual inspection, or micro cracks, which can be detected only with microscopes or non-destructive tests. Ansys has the advantage of explaining all minor cracks which could not be visually detected during loading in the experimental test. This illustrates the extensive crack in the numerical models when compared by those at the experimental study.

As illustrated in figures from 24 to 34, most cracks are flexural cracks that appeared in the middle third portion of the beam. Flexural cracks appear from the start of loading. Minor compression cracks appear at load level 0.5 P_{ult} under loading points as there are no pads were added under loading. These compression cracks increased at 0.75 P_{ult}, as well as secondary cracks this loading level. Shear cracks appear near supports at load value greater than 0.75P_{ult}. At failure all

crack types were extensively increased. Compression cracks were localized under supports at control beam at load level of 0.75 P_{ult} while existed between loading point for strengthened beam. At load of P_{ult}, the beam can no longer support additional loads as indicated by an insurmountable convergence failure where severe cracking through the entire constant moment region occurred. Also, compression cracks widely increased at the upper part of the beam due to crushing failure of the concrete.

It was found that preloading the beams did not show remarkable different behavior for the mode of failure. But all cracks especially secondary cracks at failure are dramatically enhanced. Generally, the difference between FA and C jackets in cracking patterns is not clear, because the cracking loads are compared with the ultimate load ratio for each type.

It could be concluded that Ansys is a good tool to simulate the cracking propagation and density in concrete. Hence, it serves as an appropriate index to estimate the overall deterioration level of the structure.

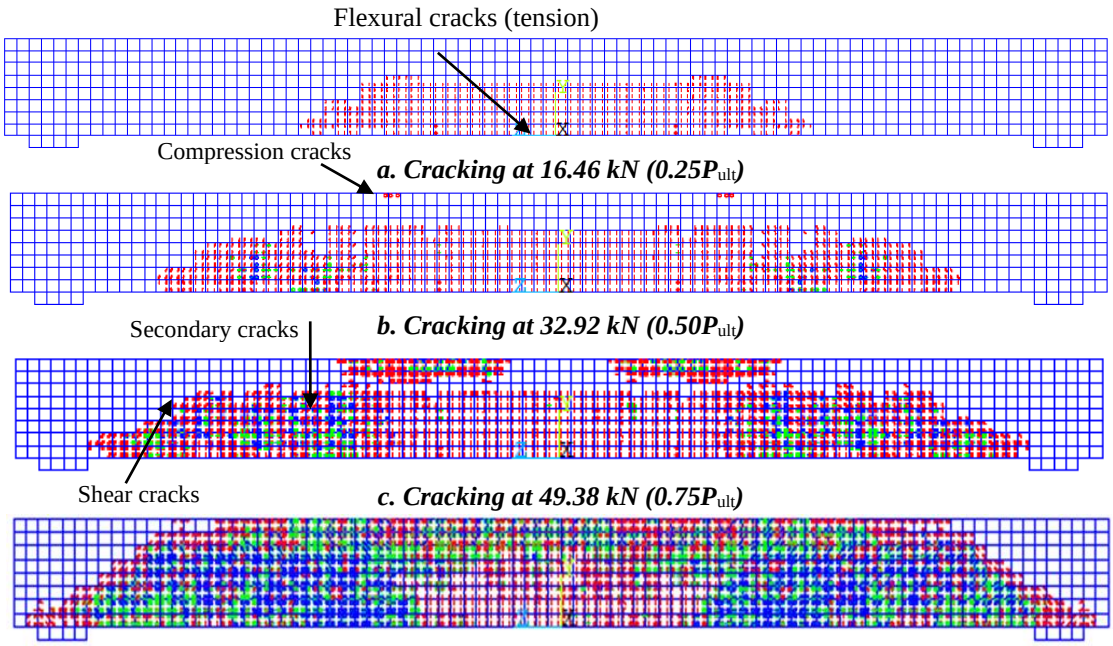

Figure 24: Crack progression for B1

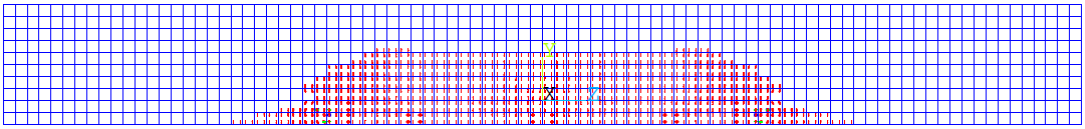

a. Cracking at 36.19 kN (0.25P_{ult})

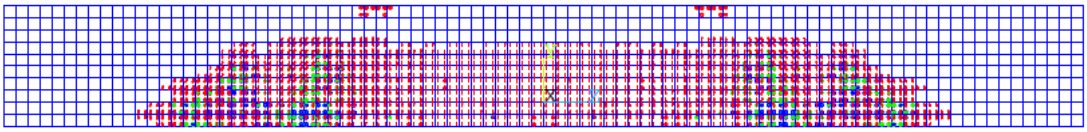

b. Cracking at 72.23 kN (0.50P_{ult})

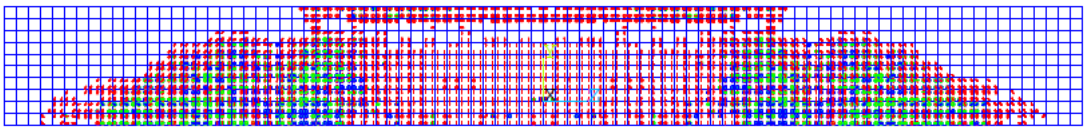

c. Cracking at 108.57 kN (0.75P_{ult})

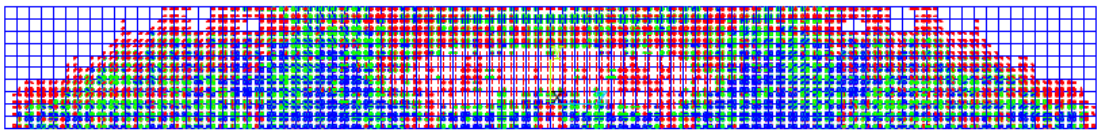

d. Cracking at 144.77 kN (P_{ult})

Figure 25: Crack progression for Beam B2

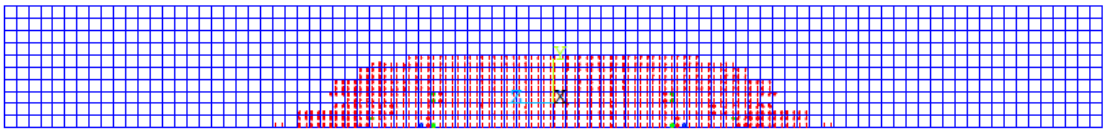

a. Cracking at 41.68 kN (0.25P_{ult})

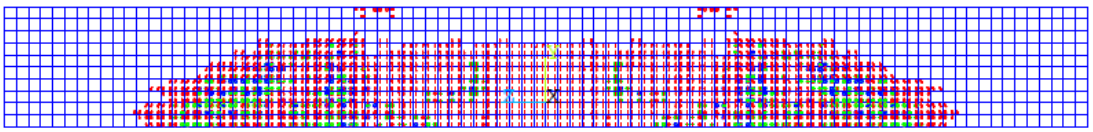

b. Cracking at 83.36 kN (0.50P_{ult})

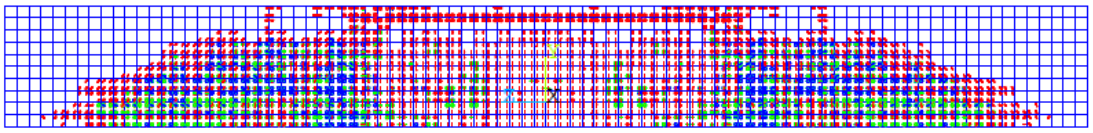

c. Cracking at 125.05 kN (0.75P_{ult})

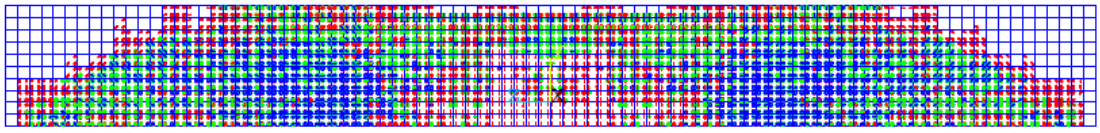

d. Cracking at 166.73 kN (P_{ult})

Figure 26: Crack progression for Beam B3

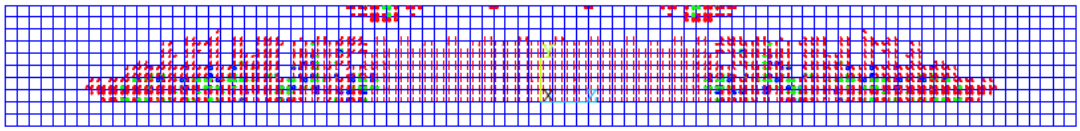

a. Cracking at 38.05 kN (0.25P_{ult})

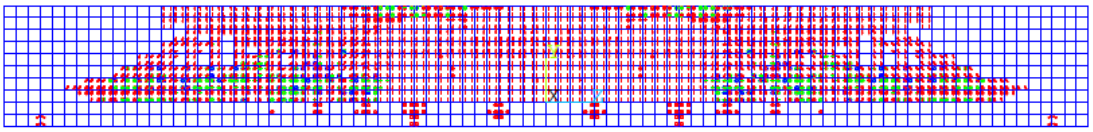

b. Cracking at 76.1 kN (0.50P_{ult})

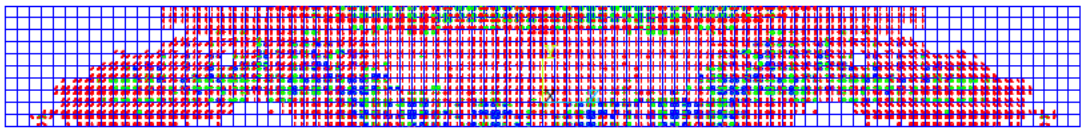

c. Cracking at 114.14 kN (0.75P_{ult})

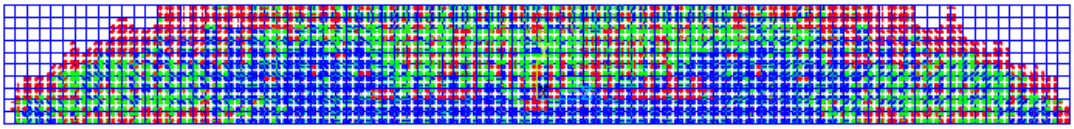

d. Cracking at 152.19 kN (P_{ult})

Figure 27: Crack progression for Beam B6

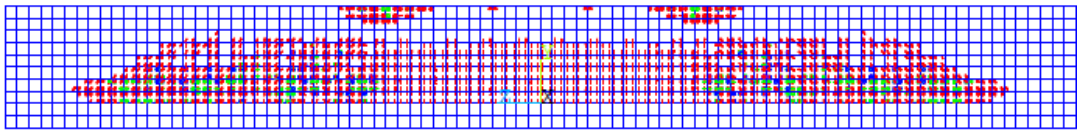

a. Cracking at 39.60 kN (0.25P_{ult})

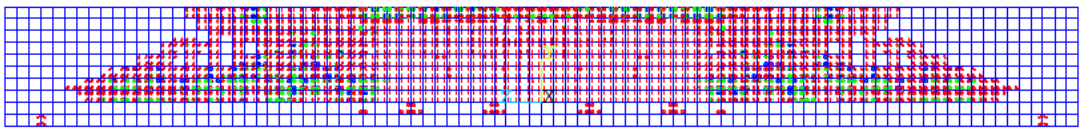

b. Cracking at 79.21 kN (0.50P_{ult})

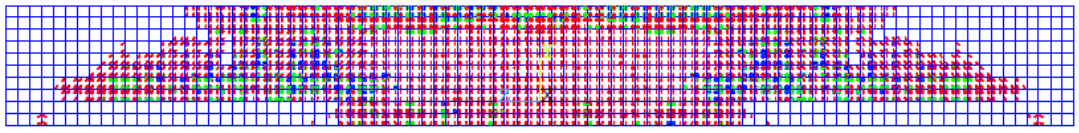

c. Cracking at 118.81 kN (0.75P_{ult})

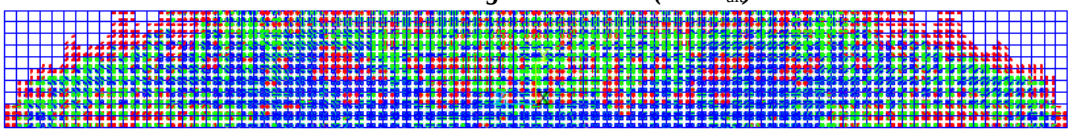

d. Cracking at 158.41 kN (P_{ult})

Figure 28: Crack progression for Beam B7

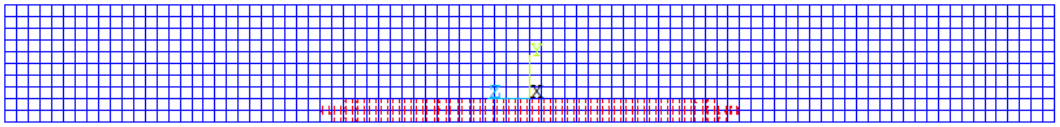

a. Cracking at 21.16 kN (0.25P_{ult})

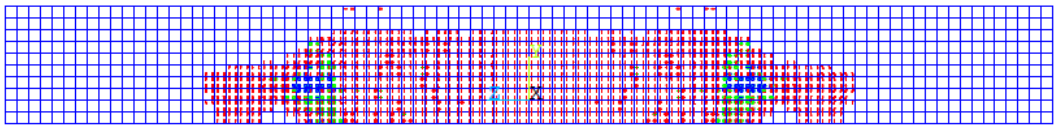

b. Cracking at 42.33 kN (0.50P_{ult})

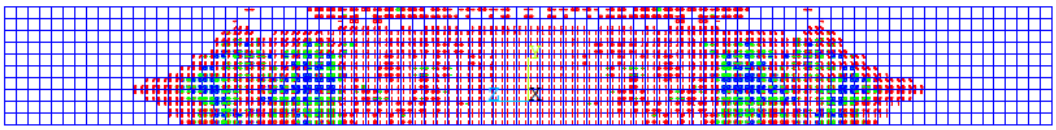

c. Cracking at 63.48 kN (0.75P_{ult})

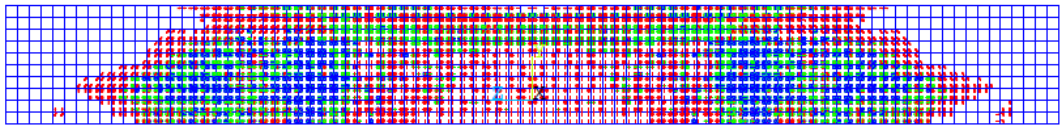

d. Cracking at 84.65 kN (P_{ult})

Figure 29: Crack progression for beam B10

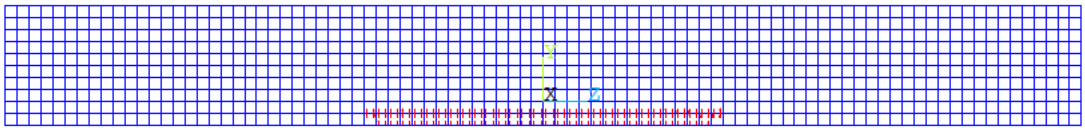

a. Cracking at 22.87 kN (0.25P_{ult})

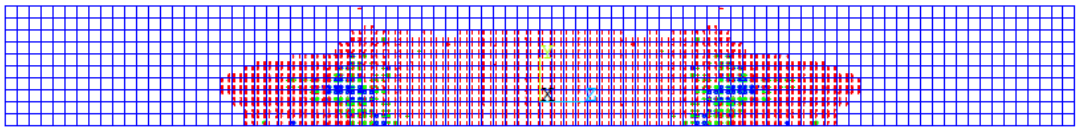

b. Cracking at 45.75 kN (0.50P_{ult})

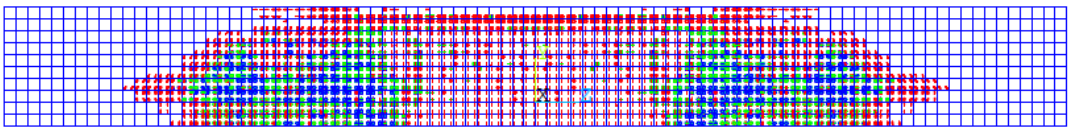

c. Cracking at 68.62 kN (0.75P_{ult})

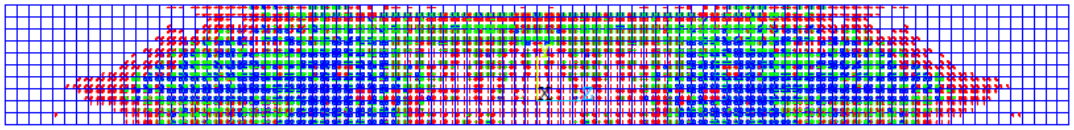

d. Cracking at 91.49 kN (P_{ult})

Figure 30: Crack progression for Beam B11

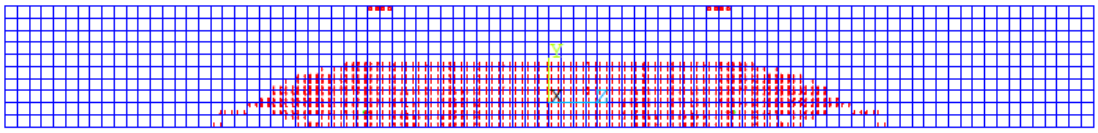

a. Cracking at 19.45 kN (0.25P_{ult})

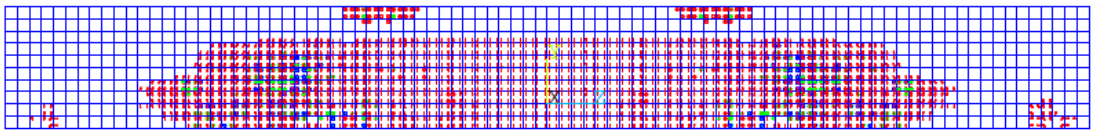

b. Cracking at 38.91 kN (0.50P_{ult})

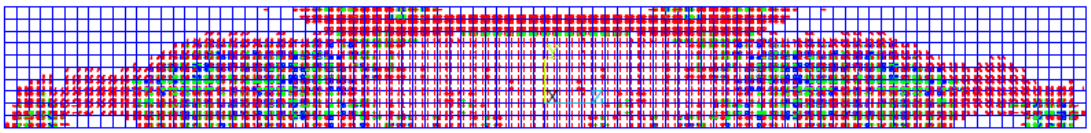

c. Cracking at 58.35 kN (0.75P_{ult})

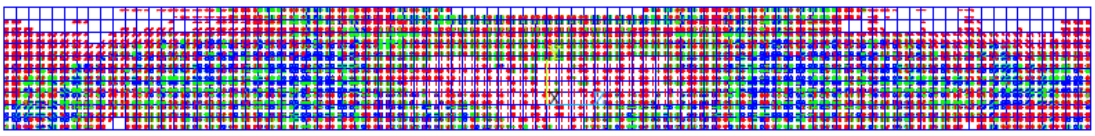

d. Cracking at 77.81 kN (P_{ult})

Figure 31: Crack progression for Beam B4

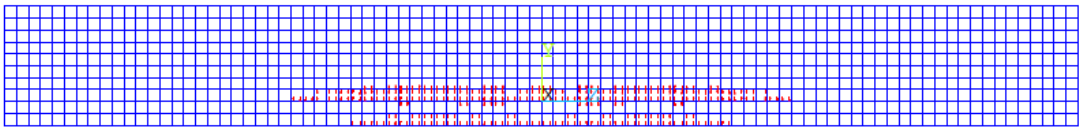

a. Cracking at 24.36 kN (0.25P_{ult})

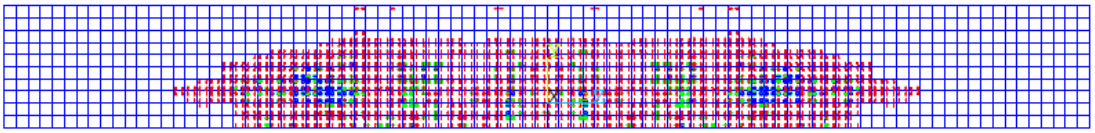

b. Cracking at 48.73 kN (0.50P_{ult})

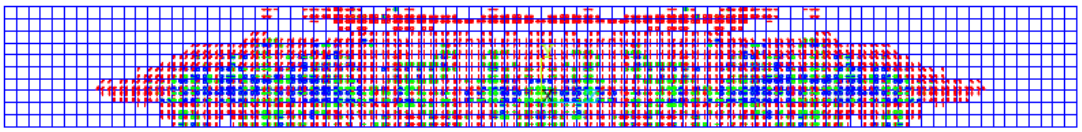

c. Cracking at 73.10 kN (0.75P_{ult})

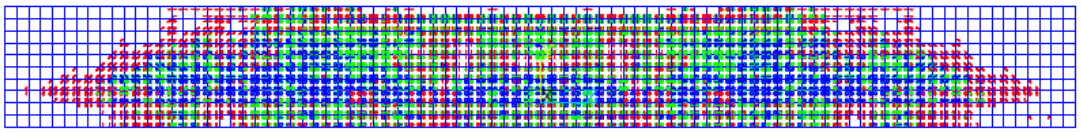

d. Cracking at 97.47 kN (P_{ult})

Figure 32: Crack progression for Beam B5

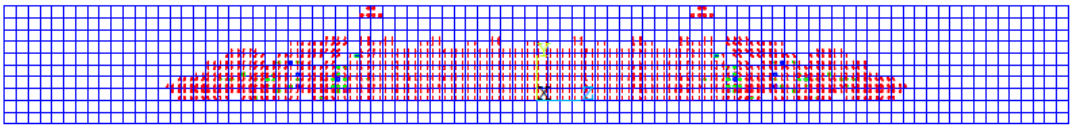

a. Cracking at 19.45 kN (0.25P_{ult})

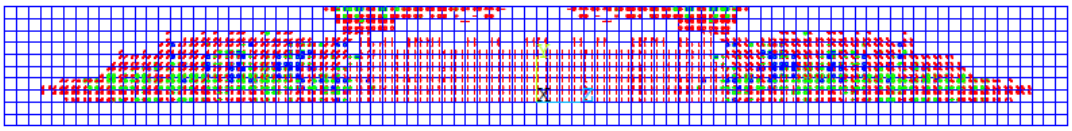

b. Cracking at 38.90 kN (0.50P_{ult})

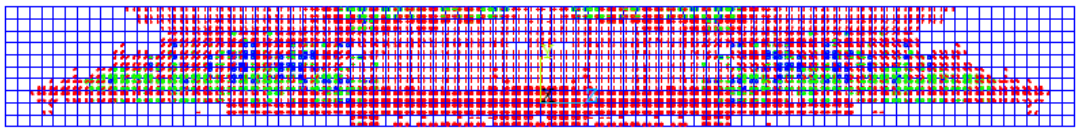

c. Cracking at 58.35 kN (0.75P_{ult})

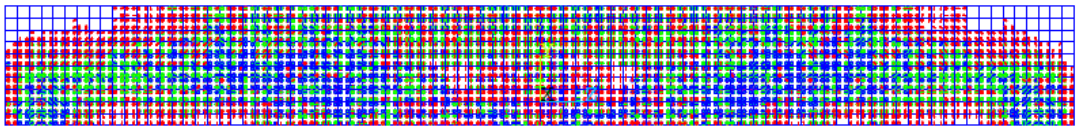

d. Cracking at 77.81 kN (P_{ult})

Figure 33: Crack progression for B13

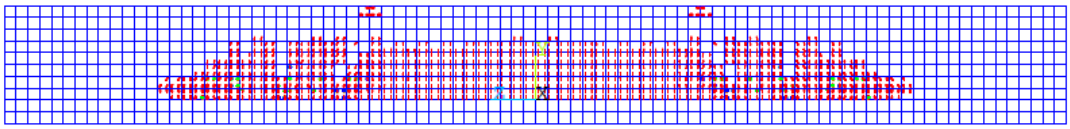

a. Cracking at 23.72 kN (0.25P_{ult})

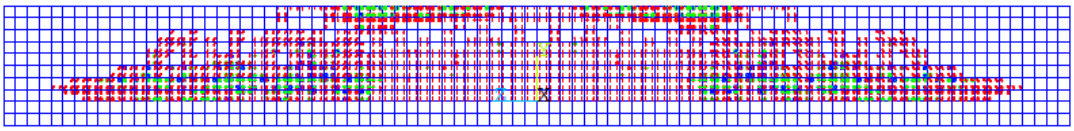

b. Cracking at 47.45 kN (0.50P_{ult})

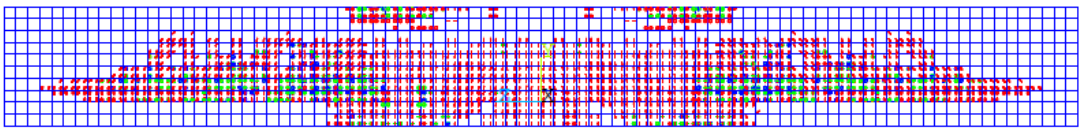

c. Cracking at 71.18 kN (0.75P_{ult})

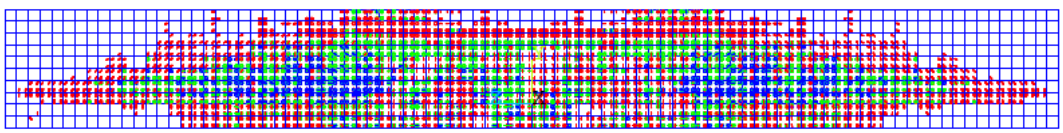

d. Cracking at 94.91 kN (P_{ult})

Figure 34: Crack progression for B14

4.4 Stresses in beams

Similarly, to the crack pattern, Ansys could clearly illustrate the variation of concrete stresses at the ultimate load level in the longitudinal Z-direction in beams and jackets as shown in Figures 35 to 45. It is clear that compressive stresses spread at the top of the beam whereas tensile stresses appeared in the bottom of the beams. It should be noted that the compressive stress of the control beam B1 was less than the compressive strength of the concrete; σc=-30.0 N/mm^2 which means that failure of the beam was due to the yield of reinforcement.

Although beams B2 and B3 have the same reinforcement, beam B3 has a higher ultimate load capacity (165.0 KN). Besides, the compressive stresses in the original beam were successfully reduced due to the higher compressive strength of FA mix and good bond between the original beam and the jacket. In addition, while reinforcement of beams and jackets are responsible for resisting tensile stresses due to flexural loads, glass fibers in FA mix help in reducing these stresses in the original beams. This is clearly illustrated in the bottom of the original beam in Figures 37 and 38.

The compressive stresses were reduced for preloaded beams by 32.1% and 15.0% when using GFA and control mixes, respectively. The compressive stresses of unreinforced jackets of beams B10 and B11 were reduced by 7.5% and 14.7 % when using FA and control mixes, respectively. For beams that were exposed to elevated temperature, the compressive stresses were increased in the original beam due to damage of the jacket.

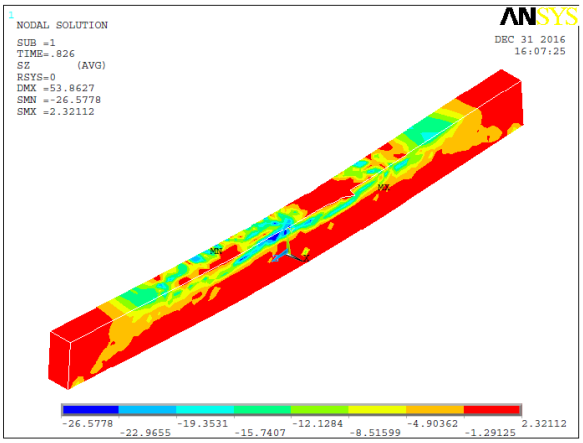

Figure 35: Contour of Normal stresses for B1 (σc=-26.5 N/mm^2)

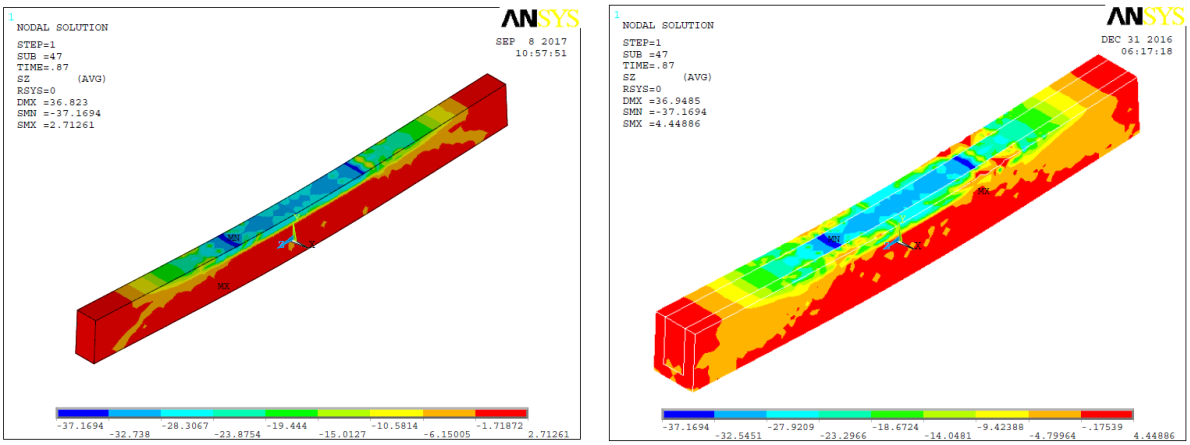

Figure 36: Contour of Normal stress for B2 (σc=-32.5 N/mm^2)

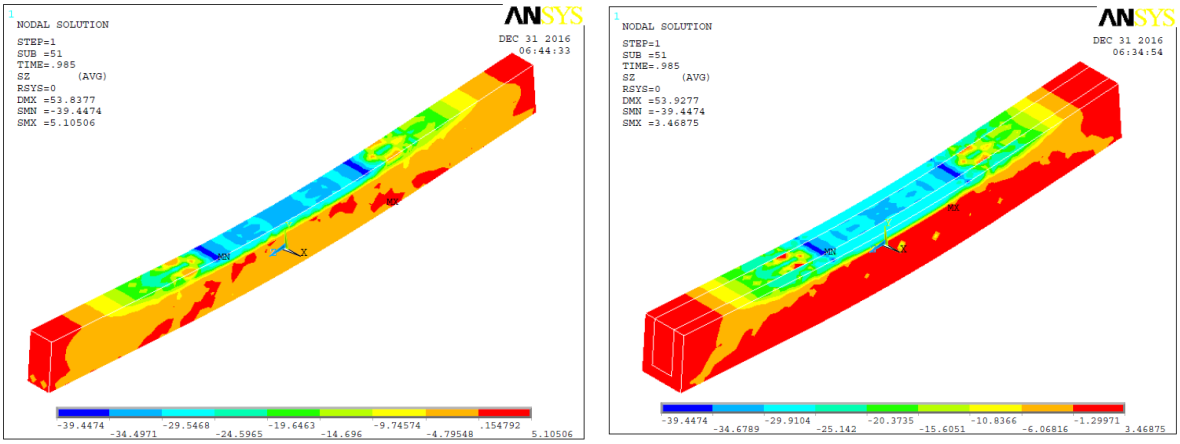

Figure 37: Contour of Normal stress for B3 (σc=-29.0N/mm^2)

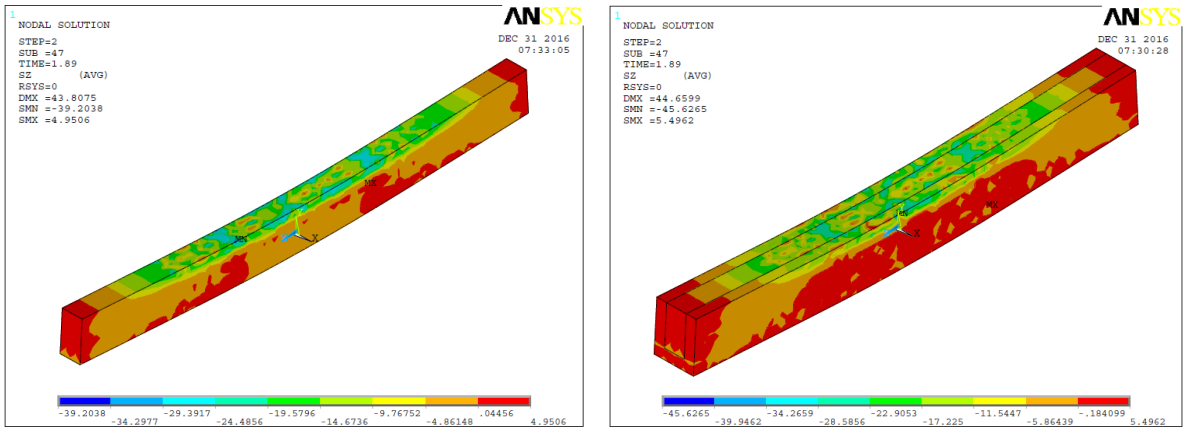

Figure 38: Contour of Normal stress for B6 (σc=-22.6N/mm^2)

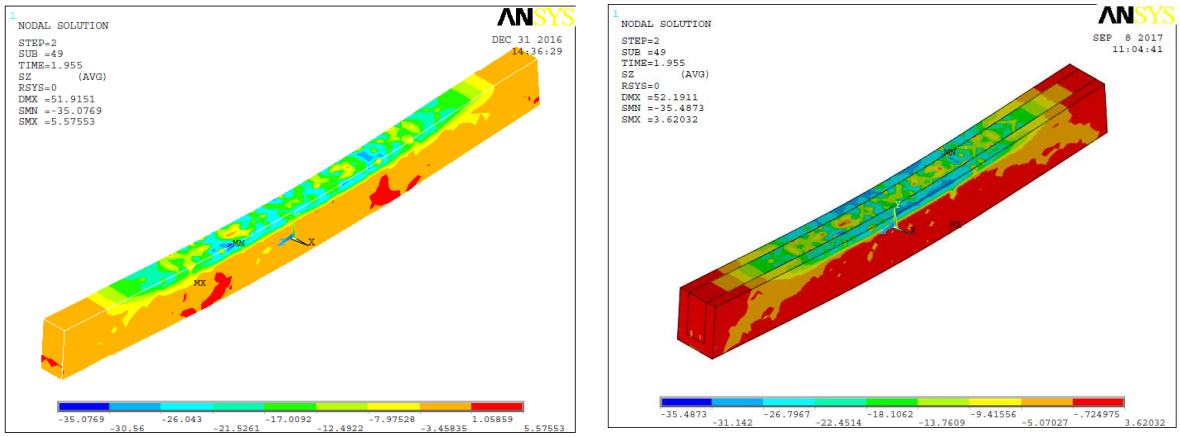

Figure 39: Contour of Normal stress for B7 (σc=-18.0N/mm^2)

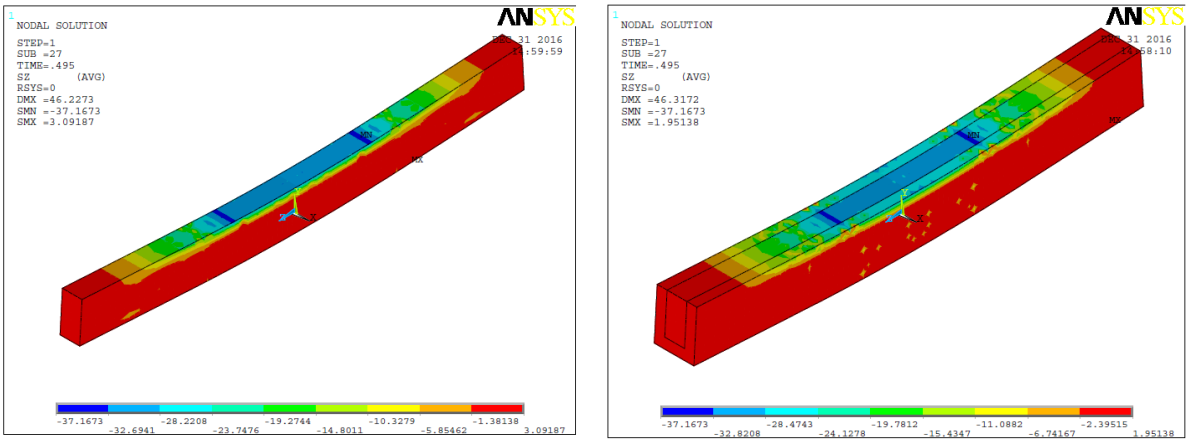

Figure 40: Contour of Normal stress for B10 (σc=-24.5N/mm^2)

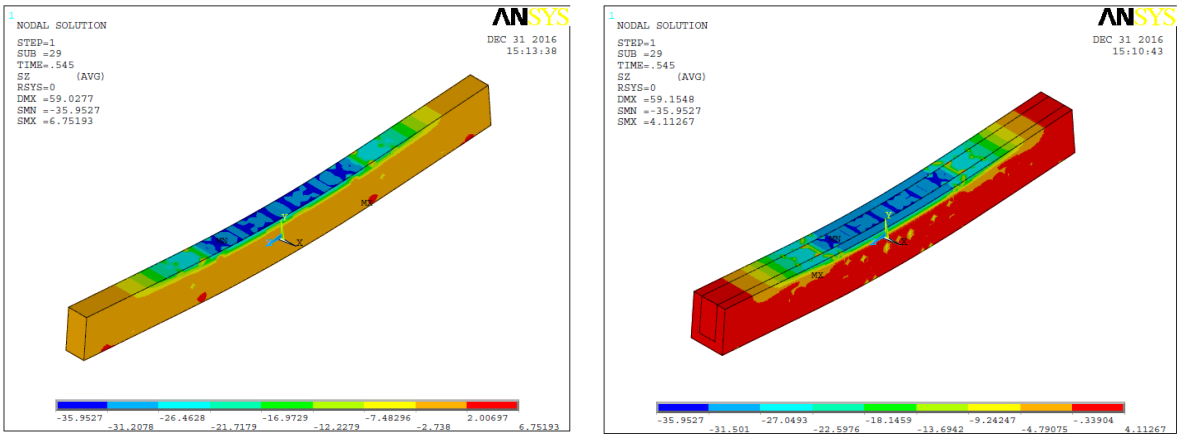

Figure 41: Contour of Normal stress for B11 (σc=-22.6 N/mm^2)

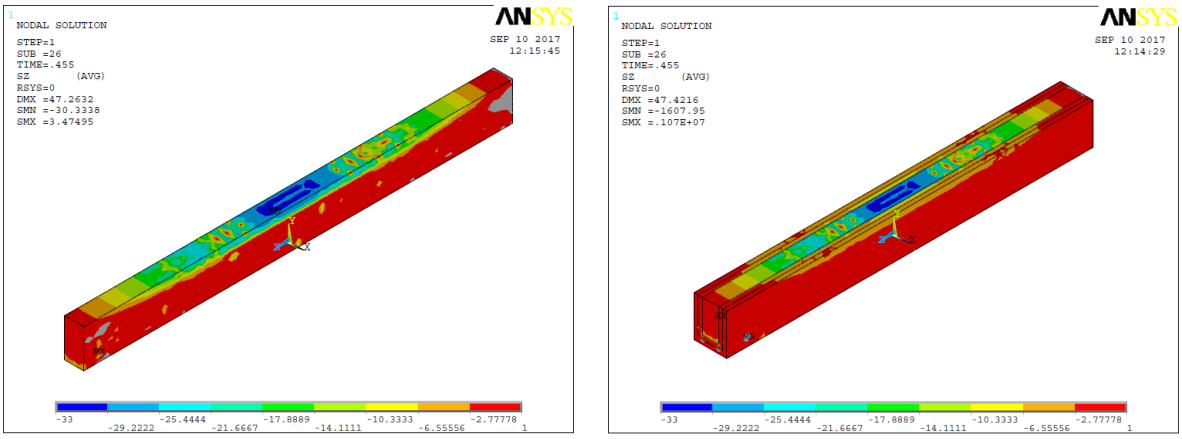

Figure 42: Contour of Normal stress for B4 (σc=--33.0 **N/mm^2)**

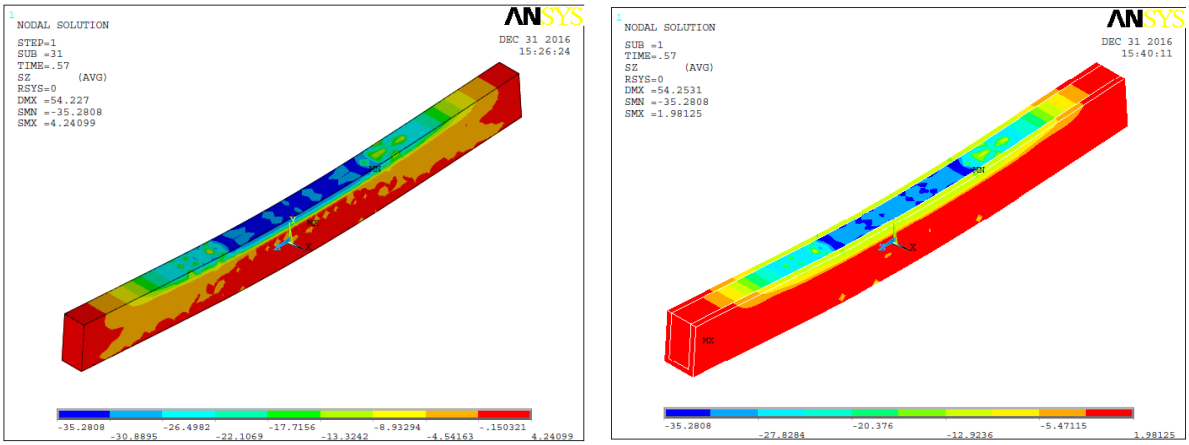

Figure 43: Contour of Normal stress for B5 (σc=-30.5**N/mm^2)**

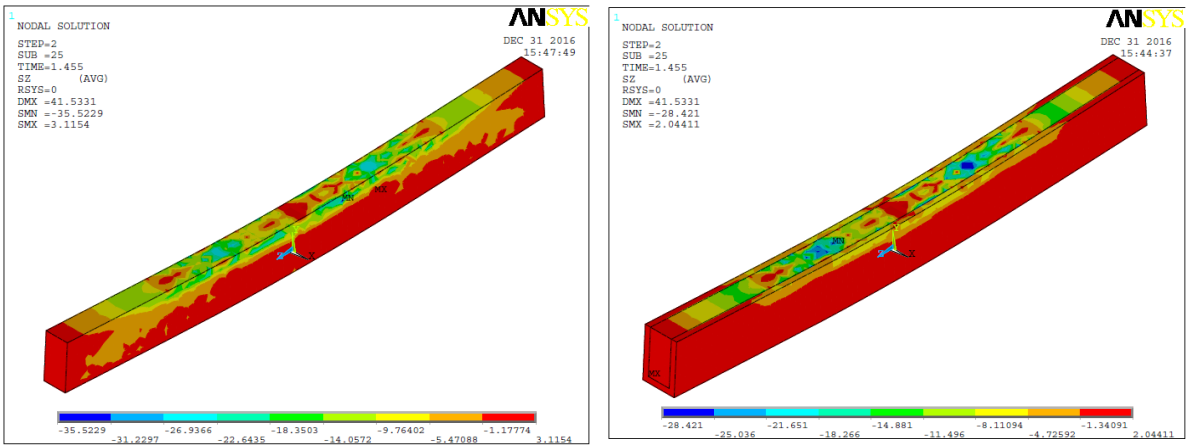

Figure 44: Contour of Normal stress for B8 (σc=-14.2 **N/mm^2)**

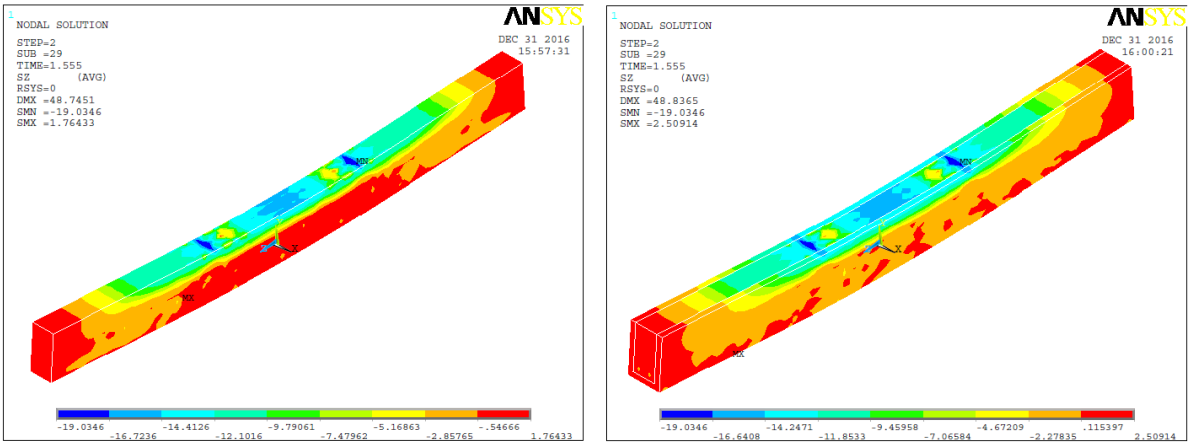

Figure 45: Contour of Normal stress for B9 (σc=-11.9 N/mm^2)

CONCLUSION

Based on the numerical results of this study, the following can be concluded:

- Good agreement between numerical and experimental results was obtained. Hence, the presented FE models showed the potential of performing numerical simulation instead of experimental tests to save time and costs.
- Reinforced jackets show superior to unreinforced ones with respect to load carrying capacity, cracking load, stiffness and ductility.
- Preloading of beams to 65% of the ultimate load of the control beam before strengthening with reinforced jackets had a minor effect on the behavior of repaired beams.
- Use of GFA mix in jackets shows better performance compared to control mix at normal temperature and after exposure to elevated temperatures. The existence of glass fibers in GFA mix enhanced the ductility index of jackets when compared by control mix.
- Elevated temperature effect was tremendous on control beams. The ultimate and cracking loads were dramatically reduced for other beams.
- Preloaded beams that used unreinforced jackets made of GFA mix showed identical behavior to reinforced jackets made of control mix after exposure to elevated temperatures. The credit goes to glass fibers and GFA mix in enhancing both stiffness and ultimate capacity.
- ANSYS has the advantage of explaining all minor cracks which could not be visually detected during loading in the experimental tests. This illustrates the extensive crack in the numerical models when compared by those at the experimental study.

REFERENCES

[1] Sachin S. Ravala, Urmil V. Dave "Effectiveness of Various Methods of Jacketing for RC Beams", Procedia Engineering. 51, pp. 230-239, 2013.

[2] Jumaat M.Z., Kabir M. H. and Obaydullah M., "A Review of the Repair of Reinforced Concrete Beams", Journal of Applied Science Research, Vol.2, No. 6, pp. 317-326, 2006.

[3] Jamil Md. A., Zisan Md. B., Alam M. R. & Alim H., "Restrengthening of RCC Beams by Beam Jacketing ", Malaysian Journal of Civil Engineering, Vol.25, No.2, pp. 119-127, 2013

[4] Hsu J. H. and Lin C. S., "Residual Bearing Capabilities of Fire-Exposed Reinforced Concrete Beams", International Journal of Applied Science and Engineering, Vol. 4, No.2, pp. 151-163, 2006.

[5] Moetaz M. E., Ahmed M. R., and Shadia E., " Effect of Fire on Flexural Behavior of RC Beams", Construction and Building Materials, Vol. 10 No. 2, pp. 147-150, 1996.

[6] Jacob B., Balaji A. and John E., "Behaviour of concrete structures under fire - a comparative study between IS 456: 2000 and finite element software ANSYS", American Journal of Engineering Research (AJER) e-ISSN: 2320-0847 p-ISSN: 2320-0936 ,Vol.3 pp.62-66, 2013.

[7] Ye Z. and Yalong, "Nonlinear Analysis of Reinforced Concrete Frame Subjected to Fire", International Conference on Mechatronics, Electronic, Industrial and Control Engineering (MEIC 2015), The authors - Published by Atlantis Press, 2015.

[8] Musmar M., "Numerical Evaluation of the Thermo-Mechanical Response of Shallow Reinforced Concrete Beams", Theor. Appl. Mech., Vol. 6, NO.1,33–47, 2013

[9] IS 456:2000, Plain and Reinforced Code of Practice, Bureau of Indian Standard.

[10] YEHIA A. Z. AND YASMIN H. A., " Effect of Elevated Temperature on RC Precracked Beams Repaired and Strengthened Using Jackets of Cementitious Materials", IJCIET, VOL. 8, NO. 091, May 2017.

[11] ANSYS, "ANSYS Help", Release 12.0, Copyright 2009.

[12] User Manual, ANSYS 12.01, USA: Ansys. Inc. Houston, 2006.

[13] Hanadi F. N., Abdulrahman Sh. Kh., Abass H. E., " Shear Behavior Of RC Beams Strengthened With Varying Types Of FRP Materials Using Finite Element Analysis, Journal of Engineering and Development, ISSN 1813-7822 183, Vol. 15, No. 1, Mar. 2011.

[14] William, K. J. and Warnke, E. p., "Constitutive Model for the Triaxial Behavior of Concrete", Proceedings, International Association for Bridge and Structural Engineering, Vol. 19, ISMES, Bergamo, Italy, 1975.

[15] Topcu I. B. and Karakurt C.," Properties of Reinforced Concrete Steel Rebars Exposed to High Temperatures", Hindawi Publishing Corporation Research Letters in Materials Science Vol. 2008, Article ID 814137, doi:10.1155/2008/814137.

[16] Habib E, Yildirim U, Eren O, Column repair and strengthening using RC jacketing: a brief state-of-the-art review, Innovative Infrastructure Solutions (2020) 5:75 https://doi.org/10.1007/s41062-020-00329-4

[17] P. Parandaman and M. Jayaraman, "Finite Element Analysis of Reinforced Concrete Beam Retrofitted with Different Fiber Composites". Middle-East Journal of Scientific Research 22 (7), 948-953, 2014 ISSN 1990-9233 , IDOSI Publications, 2014 DOI: 10.5829/idosi.mejsr.2014.22.07.21979

[18] Yaohui Shen, Longbin Lin and Zhengwei Feng , Finite element analysis of reinforced concrete beams with openings in the abdomen and strengthened with steel sleeves based on ANSYS